

## Influence of Tropical Climate Exposure on the Mechanical Properties of rHDPE Composites reinforced by Zalacca Midrib Fibers

Ariawan, Dody

Mechanical Engineering Department, Faculty of Engineering, Universitas Sebelas Maret Surakarta

Wahyu Purwo Raharjo

Mechanical Engineering Department, Faculty of Engineering, Universitas Sebelas Maret Surakarta

Diharjo, Kuncoro

Mechanical Engineering Department, Faculty of Engineering, Universitas Sebelas Maret Surakarta

Wijang Wisnu Raharjo

Mechanical Engineering Department, Faculty of Engineering, Universitas Sebelas Maret Surakarta

他

<https://doi.org/10.5109/4842526>

---

出版情報 : Evergreen. 9 (3), pp.662-672, 2022-09. 九州大学グリーンテクノロジー研究教育センター  
バージョン :

権利関係 : Creative Commons Attribution-NonCommercial 4.0 International



# Influence of Tropical Climate Exposure on the Mechanical Properties of rHDPE Composites reinforced by Zalacca Midrib Fibers

Dody Ariawan<sup>1,2</sup>, Wahyu Purwo Raharjo<sup>1,2,\*</sup>, Kuncoro Diharjo<sup>1,2</sup>,  
Wijang Wisnu Raharjo<sup>1,2</sup>, Bambang Kusharjanta<sup>1,2</sup>

<sup>1</sup>Mechanical Engineering Department, Faculty of Engineering, Universitas Sebelas Maret Surakarta, Indonesia

<sup>2</sup>Research Group of Nonmetal Processing, Universitas Sebelas Maret Surakarta, Indonesia

\*Author to whom correspondence should be addressed:

E-mail: wahyupraharjo@ft.uns.ac.id

(Received September 29, 2021; Revised June 6, 2022; accepted July 4, 2022).

**Abstract:** This study aims to investigate the influence of weather exposure on the physical and mechanical characteristics of rHDPE matrixed composites reinforced with zalacca midrib fibers. The specimens were fabricated using the compression molding method into 3 variations which include the neat rHDPE as control as well as the untreated and alkaline-treated zalacca fiber-reinforced rHDPE composites at 30 %  $v_f$ . Moreover, the weathering exposure was conducted under a tropical climate for 6 months after which all the specimens became chalky and showed significant changes in color. The FTIR results indicated that carbonyl groups of rHDPE emerged due to the weathering exposure while the thermogravimetry test showed no significant change in thermal stability. It was also discovered that their flexural and impact strength were enhanced by the alkaline treatment but the effect diminished after weathering. The micrograph observation showed some gaps between fibers and matrix, breakage of the fibers and matrix bonds, and cracks on matrix around the fibers. Furthermore, the fracture of the neat rHDPE was observed to be more brittle after exposure and this means the neat rHDPE and rHDPE-ZF composites are suitable for indoor applications but not recommended for outdoor uses.

**Keywords:** weather exposure; rHDPE, zalacca fibers; alkaline treatment; compression molding

## 1. Introduction

High quality materials are recently required to have acceptable mechanical properties appropriate to their function, competence cost of raw stock, manufacturing ability, and recyclability<sup>1)</sup>. This is the reason bio-composites consisting of natural fibers or matrices<sup>2)</sup> have become alternatives for structural panels in both buildings and vehicles panels due to some of their advantages such as low cost, high availability and biodegradability<sup>3)</sup>.

Zalacca is an Indonesian native plant with high economic values due to the fact that its fruits belong to the same family as coconut which grows as a cluster<sup>4)</sup> and the bark is covered by the leaf midribs. Zalacca midrib fiber, similar with other natural fibers such as sisal, coir, jute, ramie, kenaf, pineapple midrib fiber, and areca nut fiber<sup>5)</sup>, has the potential to be used as reinforcements of composites due to its stiffness and strength, abundance, renewability and bio-decomposition<sup>6)</sup>. Meanwhile, 2-3 midribs of this plant are usually cut every 4 months for its cultivation and need to be dumped for up to 6-8 months to decompose without treatment<sup>7)</sup>. It is important to note that

zalacca midrib waste, as an organic matter, has potency for biogas production through an anaerobic digestion process as observed in olive pomace waste in addition to its usefulness as a composite reinforcement<sup>8)</sup>. Its ash can also be used to reinforce aluminum-based composites in the same manner with groundnut shell<sup>9)</sup> while the midrib waste can be used as a source of activated carbon such as sugarcane bagasse<sup>10)</sup>.

One of the drawbacks of natural fiber is its hydrophilicity which causes high water absorption, thereby leading to poor compatibility with synthetic polymer matrix which is hydrophobic. Alkaline treatment is one of the methods usually used to modify the properties of fibers. This involves immersing the material in alkaline solution for a specific time<sup>11)</sup> in order to increase the tensile strength and elastic modulus<sup>12)</sup>, improve the physical and chemical properties<sup>13)</sup> as well as sodium bicarbonate treatment<sup>14)</sup>, and also to enhance the compatibility between fibers and synthetic polymers<sup>15)16)</sup>.

High-density polyethylene (HDPE) is one of the thermoplastic polymer most broadly utilized for home appliances and industries due to its excellent mechanical

properties<sup>17)</sup>, specifically the impact strength and relative stiffness compared to other thermoplastics<sup>1)</sup>. It is recycled as rHDPE (recycled high-density polyethylene) having comparable mechanical properties with the virgin HDPE<sup>18)</sup> and normally applied as the matrix of natural fiber composites.

The composites consisting of natural fibers and polymers depend on the fiber and polymer matrix properties and adhesion between these materials<sup>19)</sup>. A previous study conducted on the utilization of wheat straw fibers as reinforcements with the focus on the effect of weight fraction on mechanical properties of recycled polyethylene-wheat straw fiber composites showed that the tensile and flexural strength increased in weight fraction between 10 and 50 % and the highest value was achieved on weight fraction of 50 %<sup>20)</sup>.

It is important to note that the properties of composites can be affected by exposure to weather and this was confirmed by the experiment conducted on polyester-kenaf-composites for 3, 6, 9 and 12 months by Ariawan et al.<sup>21)</sup> which showed that weather influences the morphological surface and color of the composites. The FTIR test also indicated an increase in carbonyl and vinyl index while the mechanical properties reduced significantly, specifically the fracture toughness.

Umar et al.<sup>22)</sup> found that accelerated weathering has the ability to cause a drastic decrease in tensile strength after 400 h exposure while the color of composites was observed to have turned to white after 200 h and very white after 600 h of exposure. Another study by Pandey et al. focused on the effect of UV on HDPE matrixed composites using different fibers and the results showed changes in the composites color, decrease in flexural strength, and changes in the impact strength<sup>23)</sup>.

These aforementioned studies showed the possibility of using rHDPE-ZF composites for outdoor applications, specifically in the house such as the roof tiles and panels due to their high bending and impact strength. However, there is presently no in-depth study conducted to investigate the influence of weather exposure on the mechanical properties of these composites. Therefore, this study aims to analyze the effect of tropical weather exposure on the bending and impact strength as well as the physical and chemical characteristics of rHDPE-ZF composites.

## 2. Experimental method

### 2.1 Materials

Zalacca midrib was obtained from Sleman, Yogyakarta Province, Indonesia, and irregular-sized rHDPE was from a recycle shop. Meanwhile, NaOH and acetic acid were purchased from Merck® and wax mirror glaze was used to assist in removing the composites from the dies.

### 2.2 Preparation of ZFs

Midribs were cut  $\pm 30$  cm from the root and pressed by

roll-machine with  $\pm 5$  mm gap to separate their fibers. The fibers were immersed in clean water and protected from the air for 7 days up to the moment they separated and were later dried under the sun for 12 h followed by an oven at 60°C for 8 h. The dried fibers were stored in a closed container to maintain their low humidity.

### 2.3 Chemical treatment

Alkaline treatment was conducted on ZF according to the most optimum treatment as reported by Ariawan et al.<sup>24)</sup>. This involved producing the alkaline solution by mixing  $\pm 5$  wt. % NaOH and distilled water, after which the fibers cut into approximately 9-mm length were immersed in the solution for 3 h and soaked in  $\pm 1$  % acetic acid for 10 min. They were later rinsed in distilled water and dried in an oven at 60°C for 8 h to eliminate the humidity.

### 2.4 Fibers characterization

Several fiber tests were conducted before the composites fabrication to determine the mechanical properties of ZF. This involved micrograph morphology through SEM, single fiber test, crystallinity index by XRD, chemical content of ZF, the density of ZF, as well as the interfacial shear strength between ZF and HDPE. The density of samples was measured according to ASTM D792 (test method A) using a Precissa® XT 220A instrument.

The crystallinity index (CrI) values of untreated and alkaline-treated ZF were determined on a Bruker® AXS D8 Diffractometer with copper radiation with Cu K $\alpha$  ( $\lambda = 1.54$  Å) operated at 40 kW and 40 mA. Moreover, two dimensional images of ZF were obtained by capturing the image of fiber surface by using instrument model JSM-6010Plus/LV from Jeol®.

A tensile testing machine was used for single-fiber tensile and interfacial shear strength (IFSS) test using Tenso® 300 with a load cell of 30 kgf while the tensile properties of single ZF samples were evaluated in accordance with ASTM C 1557 and the IFSS specimen is prepared in line with the method used in Raharjo et al.<sup>25)</sup> which involved inserting a single fiber into the HDPE matrix with cardboard as its base.

### 2.5 Composite specimen fabrication

The rHDPE materials were washed and dried in the open air, crushed, ground and strained using 20 and 40 meshed strainers. The powdered rHDPE and ZF were mixed at 70 %:30 % of volume and 9 mm length placed in the dies and evenly lubricated using wax mirror glaze. The dies were hot-pressed using 0.268 MPa pressure and 150°C temperature for 25 min and allowed to cool at room temperature. Furthermore, the composite was removed from the dies and cut into the dimensions needed to be used as the test specimen. There were three categories of composites in this test which include neat rHDPE, as well as rHDPE composites reinforced with untreated ZF and

alkaline-treated ZF.

## 2.6 Weather exposure

The composite specimens were exposed to the weather for 1, 2, 3, 4, 5 and 6 months using an aluminum rack. The daily weather condition including humidity, rainfall rate, temperature, particulate matter (PM), ultraviolet (UV) index, and duration of sunbeam (daylight) was recorded for 6 months.

The test was performed according to ASTM D 1435 and this involved placing all specimens on the rack at an angle of 45°C, facing east, located in an open area above all other objects. Moreover, the samples were collected after 1, 2, 3, 4, 5 and 6 months of exposure to determine the degree of degradation. It is important to note that they were cleaned before the mechanical test using a towel and reconditioned in a desiccator for 24 h at room temperature.

The specimens were taken from the rack and weighed using a digital balance with  $10^{-3}$  g accuracy while their thickness was measured using a digital caliper with 0.01 mm accuracy in each month. The photographs of the composite specimens were also taken using a digital camera to obtain data on the change of color.

## 2.7 Color test

The color was tested by processing the photographs of samples taken using an android-based application known as Color Grab®. A Xiaomi® Mi5 cellular phone with 16 megapixels camera resolution was used.

## 2.8 Fourier transform infrared spectroscopy

The infrared radiation absorbed due to the vibration of chemical bonding interaction was measured through the Perkin-Elmer® spectrometer. The process involved grinding the un-weathered and weathered specimens to powder after which 5% of the 80-meshed powdered specimens mixed with 95 % KBr were passed through a disk. The absorbance spectra were measured in wavelengths ranging from 4000 to 550  $\text{cm}^{-1}$  at a resolution of 1  $\text{cm}^{-1}$  and 32 scans. Moreover, the existence of absorption peaks indicates the presence of some functional groups of specific compounds.

## 2.9 Thermogravimetric analysis and derivative thermogravimetry

TGA and DTG were conducted using a Linseis® type STA PT 1600 analyzer equipped with nitrogen as a purge gas. Approximately 15 – 20 mg of powdered sample was laid on a platinum pan and heated from 30°C to 500°C at a rate of 5°C/min.

## 2.10 Flexural test

The flexural strength of the weather-exposed specimens was tested using the three-point bending method according to ASTM D790 standard. The flexural strength and flexural modulus were also calculated using Eq. (1)

and (2), respectively.

$$\sigma_b = \frac{3FL}{2bd^2} \quad (1)$$

$$E_b = \frac{L^3F}{4bd^3y} \quad (2)$$

## 2.11 Impact test

Impact test was conducted using Izod method in accordance with ASTM D5941 standard with the focus on the specimens exposed to the weather for 1 – 6 months and the total energy absorbed by the specimen and impact strength were calculated using Eq. (3) and (4), respectively<sup>26)</sup>.

$$W = w.R.(\cos \beta - \cos \alpha^l) \quad (3)$$

$$\alpha = \frac{W}{bd} \cdot 10^3 \quad (4)$$

## 2.12 Scanning electron microscopy

SEM was used to examine the surface fracture of flexure-tested specimens using a Carl Zeiss® type Evo 10 scanning electron microscope instrument with 100-250 V voltage and 50-60 Hz frequency. It is important to note that the samples were coated with gold by a plasma sputtering apparatus at a pressure of 2 mbar for 1 min before SEM observation.

# 3. Results and discussion

## 3.1 Fiber characteristics

Fig. 1 shows the micrograph of the ZF surface after the alkaline treatment with the Fig. 1 (a) observed to indicate an extremely heterogeneous surface with several rough and smooth portions showing impurities, wax and fatty substances<sup>12)</sup>. Conversely, the alkaline treatment in Fig. 1 (b) removes these impurities to produce a cleaner fiber surface. The surface of the alkaline-treated ZF also has groove-like structures due to the removal of the cementing materials and this was confirmed by the FTIR analysis conducted by Raharjo et al.<sup>13)</sup> which showed that the partial elimination of some chemical groups is due to hemicellulose and lignin. The presence of groove-like structures has the ability to cause better interfacial adhesion and to promote friction between the materials as shown in the IFSS results in Table 1<sup>27)</sup>. Furthermore, the enhancement of IFSS shortened the critical length of ZF using Eq. (5)<sup>26)</sup> as indicated in Table 1.

$$l_c = \frac{\sigma_{ud}}{2IFSS} \quad (5)$$

Table 1 shows the changes of diffraction spectra after the alkaline treatment and the crystallinity index of alkaline-treated ZF was observed to have become higher due to the removal of amorphous material as seen in SEM results which led to an increase in crystal-packing order and density in alkaline treated ZF. This is in line with the findings of previous studies<sup>21)-22)</sup> that a partial loss of cementing material such as hemicellulose and lignin after

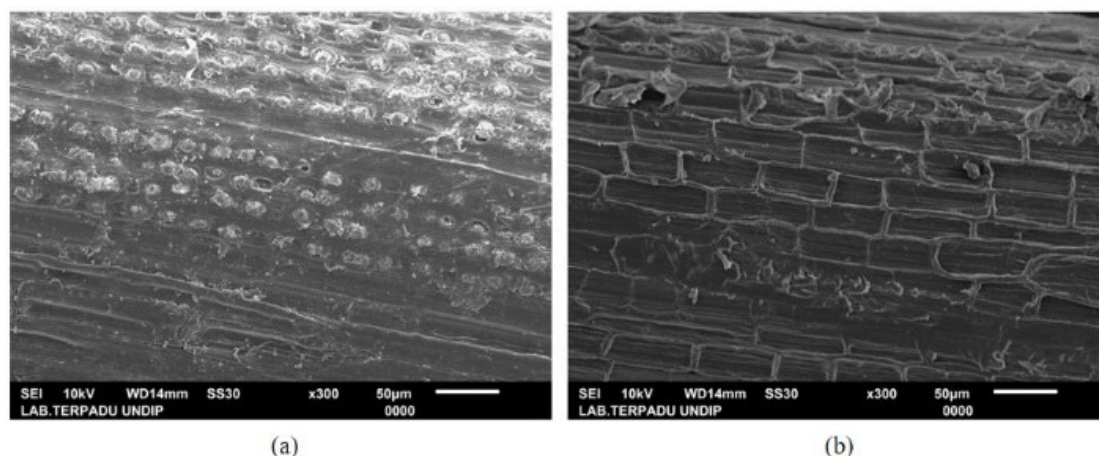


Fig. 1: Surface morphology of: (a) untreated ZF; and (b) alkaline treated ZF

alkaline treatment increased the percentage of crystallinity index. Another study<sup>13)</sup> also reported the changes in the sisal and flax crystallinity through alkaline treatment. Meanwhile, the increase of the crystallinity index indicates the improvement in the cellulose structure which further contributes to the enhancement of the tensile strength for ZF as presented in Table 1.

Table 1. Density, crystallinity index, tensile properties, interfacial shear strength (IFSS) of ZF - HDPE, and critical length of ZF

Fiber	Unit	Untreated ZF	Alkaline treated ZF	Ref.
Density	(g/cm <sup>3</sup> )	1.28 ± 0.02	1.35 ± 0.03	27)
CrI	(%)	56.14	59.88	
Tensile Strength	MPa	114.81 ± 18.04	290.66 ± 55.60	
Elastic Modulus	GPa	8.37 ± 2.67	24,38 ± 3.64	
IFSS	MPa	0.31 ± 0.10	1.01 ± 0.48	
Critical Length	mm	91.87	71.83	

### 3.2 Weather exposure

The weathering was conducted from August 2019 to January 2020 and the data recorded in Table 2 shows a significant difference in the rainfall rate but August-September had no rainfall due to the dry season while the rate is high in December-January because it is rainy season. The difference in the rainfall rate was also observed to be influenced by humidity and daylight with the value increasing with air humidity and reducing with daylight. Meanwhile, the particulate matter, UV index, and temperature tended to fluctuate insignificantly.

### 3.3 Color change of specimens

There was a color change on the specimen surfaces during direct exposure as shown in Figure 2. It was

discovered that longer exposure to sunshine led to brighter specimen color followed by chalking. This indicates the degradation of composites due to UV rays and the percentage is presented in Fig. 3 (a), (b) and (c) for neat rHDPE, rHDPE-ZF composites with alkaline treatment, and without treatment, respectively.

Table 2. Monthly weather data

Months	Rainfall rate (mm)	Relative humidity (%)	Particulate matter (PM10)
August	0.00	77.14	65.81
September	0.00	77.44	56.23
October	0.58	78.77	57.48
November	5.47	80.38	57.20
December	12.97	84.24	59.29
January	2.80	82.48	58.77
<b>Average</b>	<b>3.64</b>	<b>80.08</b>	<b>59.13</b>

Day light (%)	Maximum UV index	Average temperature (°C)
73.92	8.94	26.75
73.03	10.63	28.03
72.39	9.90	28.99
65.88	9.33	29.32
44.91	8.23	27.86
55.68	10.17	28.43
<b>64.30</b>	<b>9.53</b>	<b>28.23</b>

Source: Research and Development Center of Agriculture Faculty, Universitas Sebelas Maret

The visible components of color were R (red), G (green), B (blue), grayscale, lightness and darkness with the R, G, B, grayscale and lightness observed to have increased along with the time of exposure while the darkness decreased. This conformed with the study of

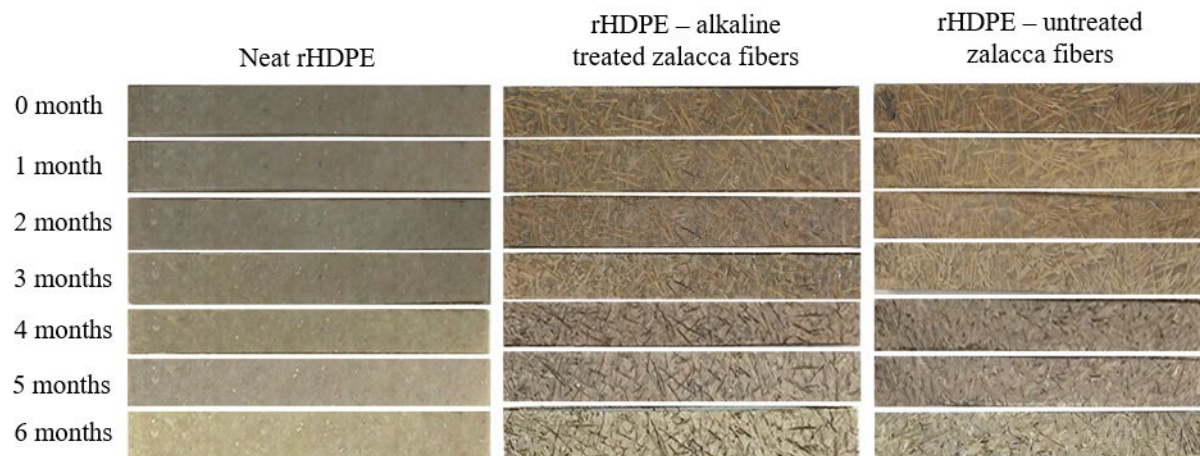


**Fig. 2:** The color change of specimens during the weather exposure

Rowell et al.<sup>29)</sup> on aspen fibers reinforced polypropylene composites which showed a chalking layer on the polymer surface after weathering for 150-200 h. This means the rate of chalking depends on the composite fabrication process, weather variable and UV intensity. The effect of UV radiation was generally observed on the composite surface because UV light was unable to penetrate 75  $\mu\text{m}$  into the composite. Moreover, there was an energy transfer process from one molecule to another leading to the production of new free radicals which migrated to the inner section of the composite and caused the color change reaction<sup>30)</sup>.

### 3.4 Fourier transform infrared spectroscopy

FTIR spectra were used to investigate the photocatalytic degradation in rHDPE during weathering as shown in Fig. 4. The neat HDPE had peaks at  $1460\text{ cm}^{-1}$  (bending deformation of  $-\text{CH}_2-$ ),  $2919$  and  $2857\text{ cm}^{-1}$  (asymmetric stretching of  $\text{CH}_2$ ) and  $719\text{ cm}^{-1}$  (swing deformation of  $\text{CH}_2$ )<sup>31)</sup>. Meanwhile, the spectrum of polyethylene film showed new peaks after radiation at  $1713$  and  $1178\text{ cm}^{-1}$  caused by carbonyl groups (stretched  $\text{C}=\text{O}$  and  $\text{C}-\text{O}$ )<sup>28)</sup>. It was also discovered that FTIR spectra

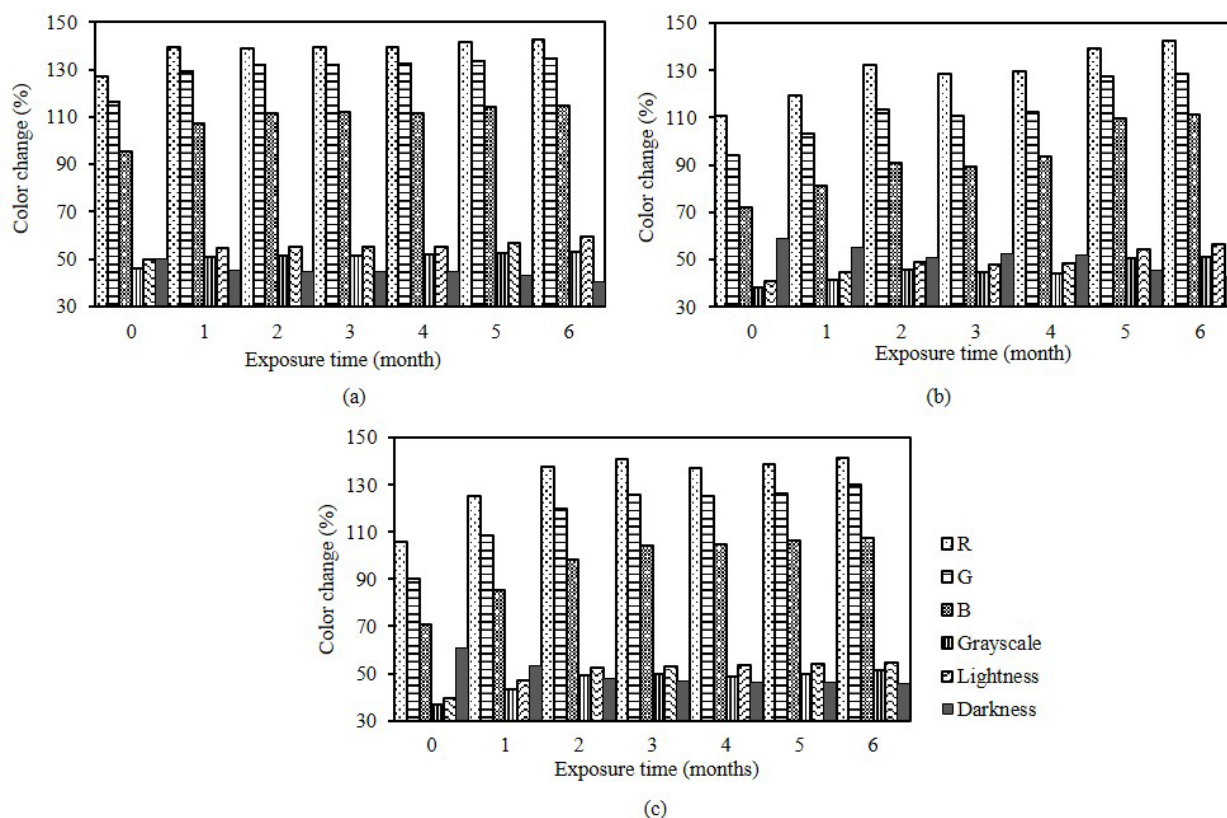


**Fig. 3:** The percentage of color change on: (a) rHDPE; (b) alkaline treated ZF composites; and (c) untreated ZF composites



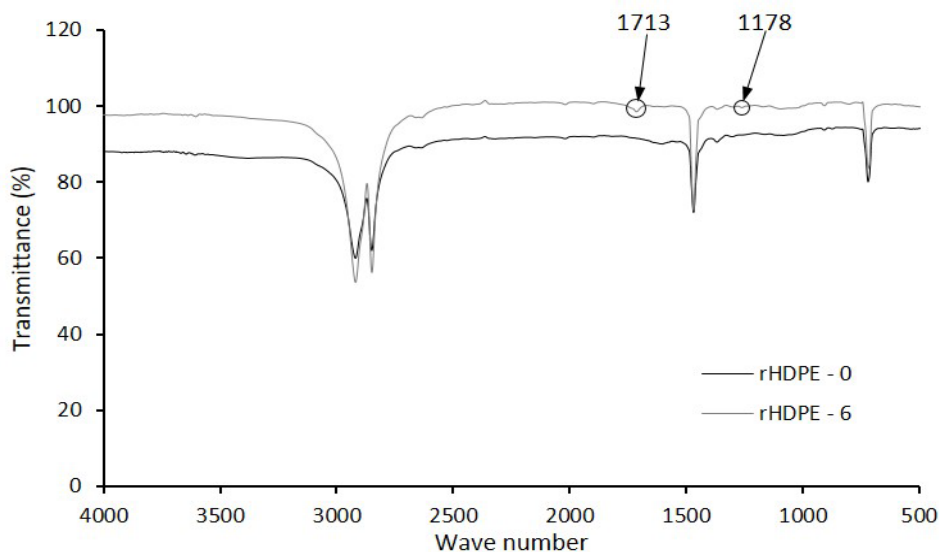


Fig. 4: FTIR spectra of rHDPE before weathering and after weathering for 6 months

of neat rHDPE had peaks at 2919.39, 2849.95, 1469.82, 1369.52 and 721.41  $\text{cm}^{-1}$ , respectively, and this indicates the existence of C-H groups according to Mouallif et al.<sup>31)</sup>. Moreover, different spectra were observed after weather exposure for 6 months in 1713.83  $\text{cm}^{-1}$  as indicated in the carbonyl group. This was in line with Asghar et al.<sup>32)</sup> that the scission of HDPE molecular chains produced free radicals. The chain scissions also degraded the mechanical properties or color change as previously discussed<sup>29)</sup>.

### 3.5 Thermogravimetric analysis

The analysis of thermogravimetry (TGA) and derivative of rHDPE before and after 6 months exposure is presented in Fig. 5, while the temperature of 95% weight loss, onset temperature, maximum decomposition temperature, and maximum derivative weight for rHDPE are shown in Table 3. It was discovered that the change in temperature of 95%, onset temperature, maximum decomposition temperature, and maximum derivative weight before and after weather exposure for 6 months failed to exceed 0.45, 0.219, 0.207 and 0.125%,

respectively, and this means there was no significant change in the thermal stability of rHDPE after 6 months of exposure.

The TGA analysis was done only for the neat rHDPE due to its role as matrix phase that is continuous or completely surrounds, and protects the other phase<sup>26)</sup>. The zalacca fibers were added to reinforce the matrix and covered by rHDPE matrix that directly exposed to sunrays.

Table 3. Temperature of 95% weight loss, onset temperature, maximum decomposition temperature and maximum derivative weight for rHDPE

Time of exposure	Month	0	6
Temperature of 95%	°C	444	446
Onset temperature	°C	456	457
Max decomposition temperature*	°C	482	483
Max derivative weight *	%/min	-0.56	-0.49

\* Data are taken from DTG

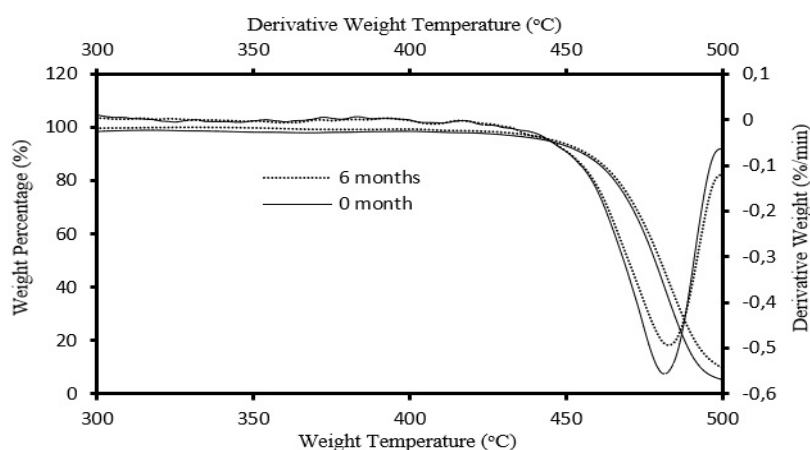
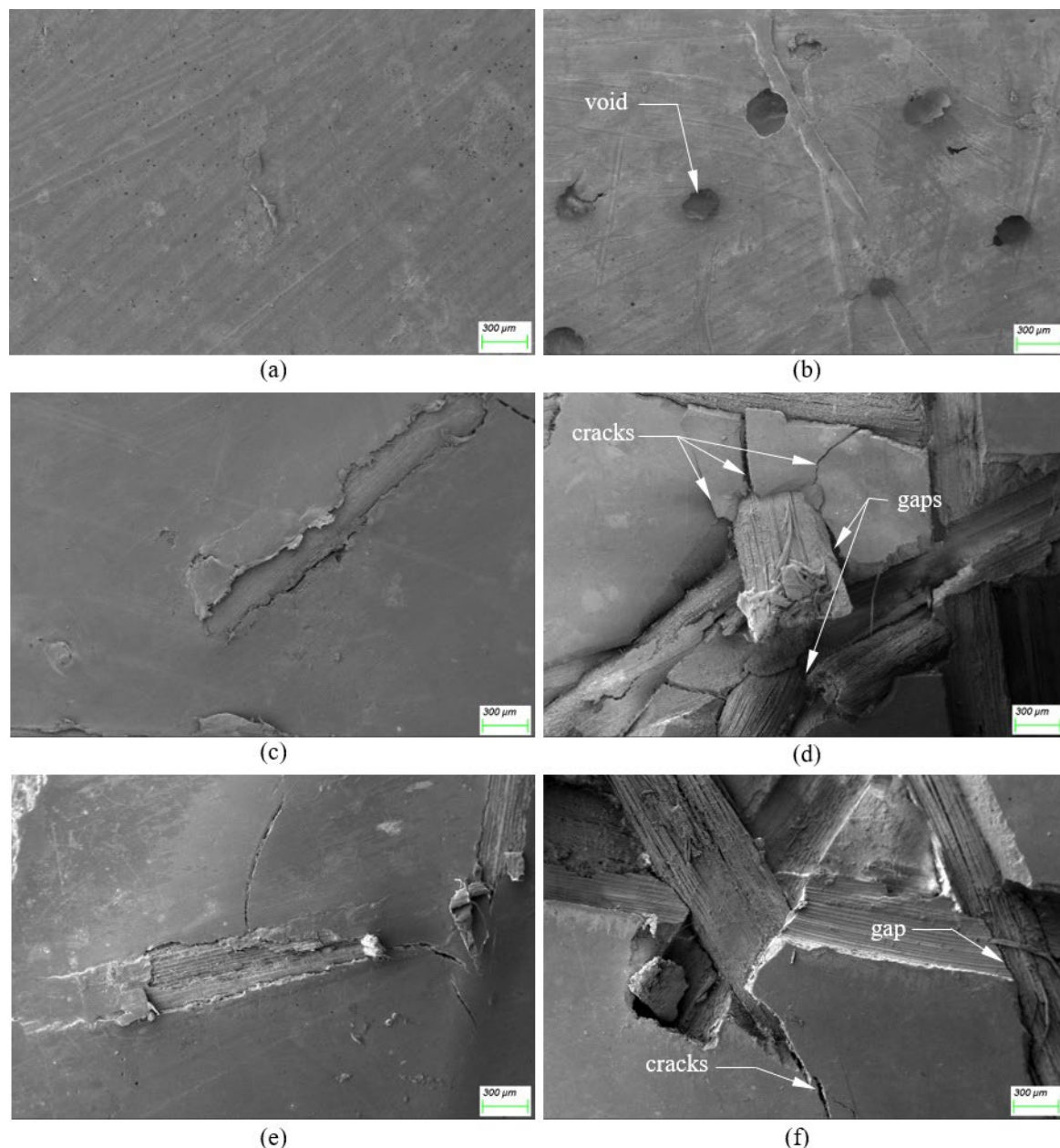


Fig. 5: TGA and DTG curve of rHDPE before and after weather exposure for 6 months



**Fig. 6:** Surface morphology of: (a) rHDPE before exposure; (b) rHDPE after 6 months exposure; (c) rHDPE/alkaline treated ZF composites before exposure; (d) rHDPE/alkaline treated ZF composites after 6 weeks exposure; (e) rHDPE/untreated ZF composites before exposure; and (f) rHDPE/untreated ZF composites after 6 months exposure

### 3.6 SEM examination of the specimen surface

Fig. 6 shows the surface morphology of neat rHDPE, alkaline-treated, and untreated ZF composites, respectively, before weathering and after 6 months exposure. Fig. 6 (a) indicates that the specimen surface was smooth without flaws before the exposure to weather. Meanwhile, there was no visible damage on the exposed surface as indicated in Fig. 6 (b) and the chalking color on the surface failed to be detected by SEM observation.

The weather-exposed composites surface was observed to be highly damaged and had some crevices, cracks and gap growths between fibers and matrix due to the combinations of several factors such as the moisture swelling in fiber, daily thermal cycles, and photo-

degradation from UV radiation of sunrays. Moreover, the thermal cycles and moisture swelling caused the expansion and shrinkage in fibers-matrix interface simultaneously. This led to the stress of the interfacial area and also induced the breakage of interfacial bonds and the matrix cracking around the fibers.

### 3.7 Flexural test

The flexural strength and flexural modulus are displayed in Fig. 7 (a) and (b), respectively. Fig. 7 (a) shows that the flexural strength of all specimens significantly decreased along with the time of weather exposure with rHDPE specimens observed to have the highest flexural strength followed by alkaline- treated and



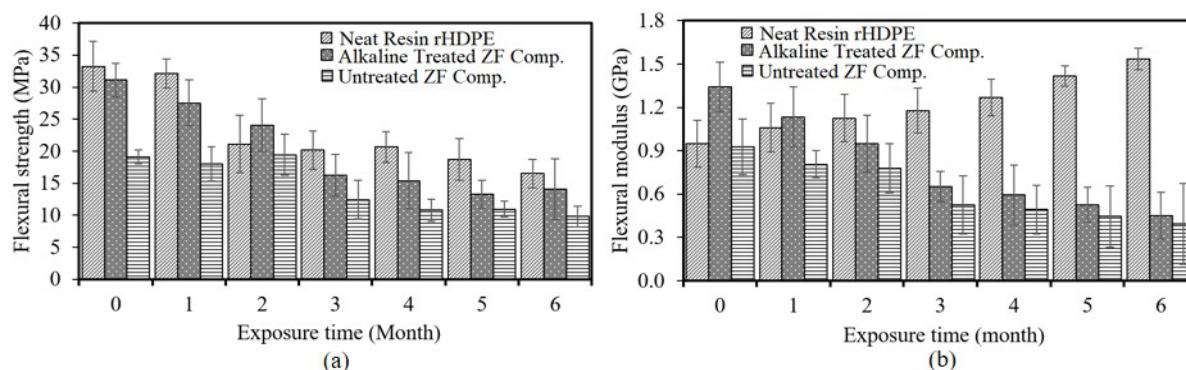


**Fig. 7:** (a) Flexural strength; and (b) flexural modulus of rHDPE, rHDPE/alkaline treated ZF composites and rHDPE/untreated ZF composites

untreated composite. This was associated with the better mechanical interlocking between the fibers and rHDPE matrix caused by the cemented components elimination through the alkaline treatment as previously discussed.

There was a different tendency in flexural modulus indicating that the observed value for the neat rHDPE increased while for both the alkaline-treated and untreated composite decreased as indicated in Fig. 7 (b). This was attributed to the existence of fibers in the composite which caused larger elongation with exposure time. However, the enhancement of the neat rHDPE after exposure was due to the photo-degradation as reported in FTIR which led to a lower deflection and induced higher elastic modulus. This was in line with the findings of Umar et al.<sup>22)</sup> that reported similar results in HDPE exposure using the accelerated weathering method. A decrease was also reported in the elastic modulus of kenaf fiber-reinforced composites due to several factors such as the interfacial debonding between fibers and matrix, decay of composites component through photo-degradation, water uptake, and thermal exposure during weathering.

### 3.8 Impact test

Fig. 8 shows the results of the impact test conducted on the samples and the impact strength of all the specimens were discovered to considerably decrease along with the exposure time. This means the increase in rHDPE brittleness was due to the chain scission during the photo-

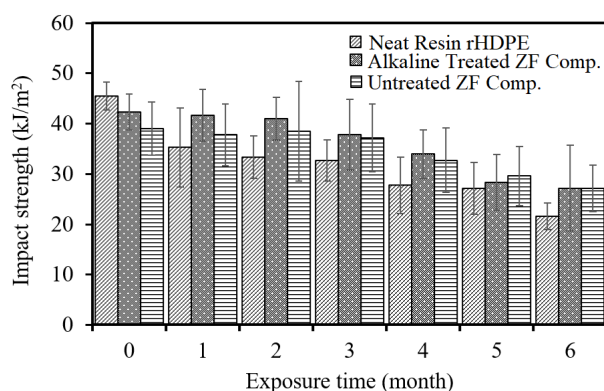


**Fig. 8:** Impact strength of rHDPE, rHDPE/alkaline treated ZF composites and rHDPE/untreated ZF composites

degradation process<sup>33)</sup>. It is also important to note that the value for rHDPE reduced significantly and was lower than the composites after the first month of exposure with the lowest recorded to be 52.52% while the alkaline-treated and untreated composites had higher values. This means the addition of fibers to both untreated and alkaline-treated was able to maintain the impact strength. The alkaline treatment also played a role at the beginning of exposures but its effect was eliminated after 2 months of exposures and this is the reason it had a similar value with the untreated composites at approximately 27 kJ/m² after 6 months of exposure.

### 3.9 Fracture surface observation

The fracture surface of the samples was observed using a scanning electron microscope as shown in Fig. 9. The specimens used for flexural test before and after 6 months weathering exposure were employed as indicated in Figs. 9 (a) and (b) for neat rHDPE, respectively. It was discovered that this specimen had an elastic fracture in accordance with the high flexural strength recorded in Fig. 7 (a). Meanwhile, Fig. 9 (b) shows a nearly flat surface and this shows the brittle fracture of the specimen.

The fracture morphology of alkaline-treated and untreated ZF composites before exposure is presented in Figs. 9 (c) and (e), respectively, and the breakage of the composite was observed to be dominant caused by the failure of fibers supporting the load transferred by the rHDPE matrix due to the existence of fiber fracture. Moreover, the fracture of weather-exposed composite for 6 months is indicated in Figs. 9 (d) and (f) for alkaline-treated and untreated ZF composite, respectively, and they were discovered to have a similar fracture due to the brittleness of fiber and gap growths caused by the environment and weather exposures. The thermal cycles and moisture absorption also induced the cycle of expansion along with the shrinkage of fiber and matrix during exposures. It is important to note that the asynchronous expansion and shrinkage enhanced the growth of the gap between fiber and matrix as well as the microcrack in the matrix.

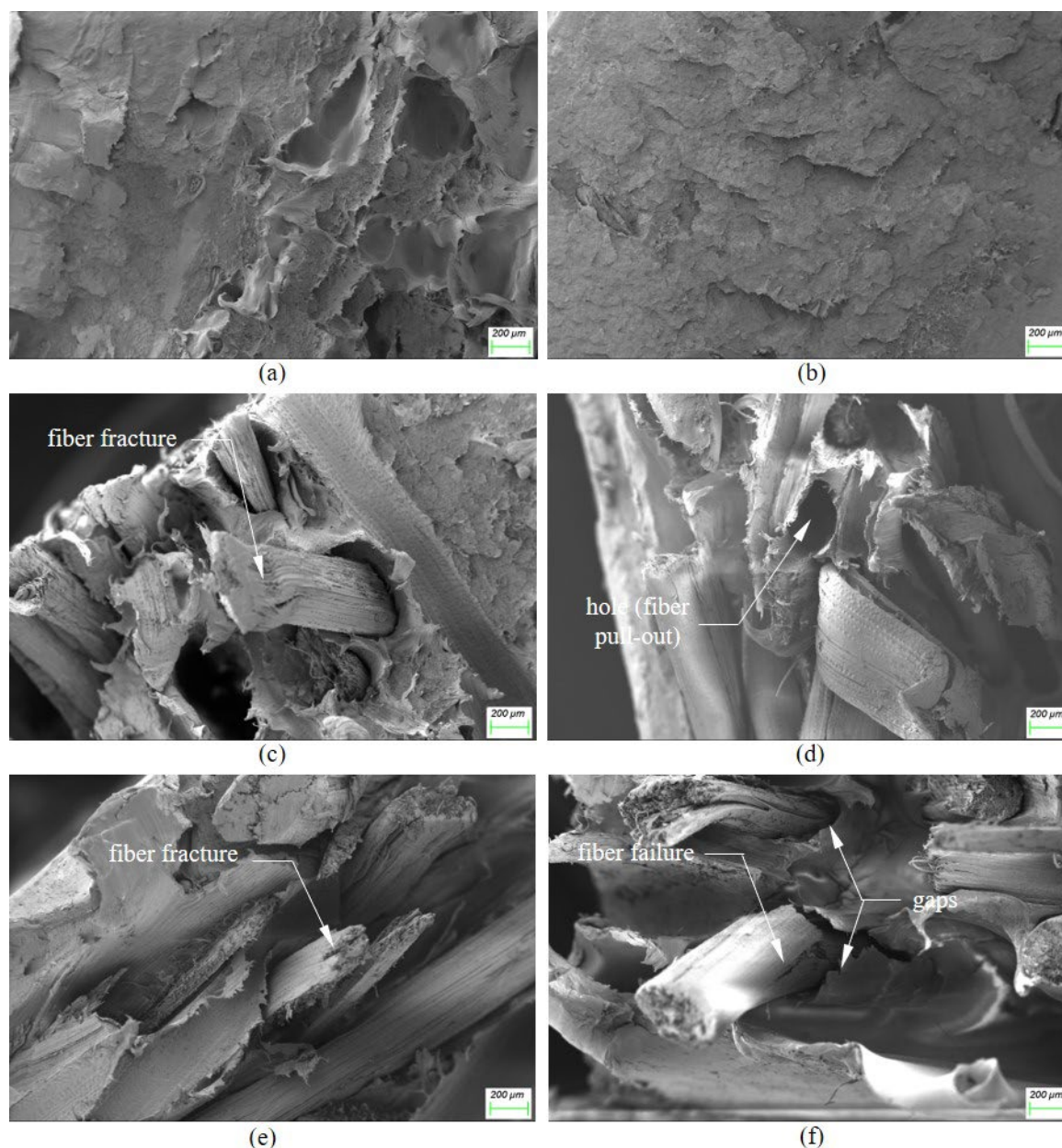


**Fig. 9:** Fracture morphology of: (a) rHDPE before exposure; (b) rHDPE after 6 months exposure; (c) rHDPE/ZF composites with alkaline treatment before exposure; (d) rHDPE/ZF composites with alkaline treatment after 6 weeks exposure; (e) rHDPE/ZF composites without treatment before exposure; and (f) rHDPE/ZF composites without treatment after 6 months exposure

#### 4. Conclusion

The neat rHDPE, untreated, and alkaline-treated ZF composites were discovered to become chalky along with the exposure time. Moreover, the damage of the neat rHDPE and rHDPE-ZF composites due to photo-degradation was verified using FTIR. This indicates the presence of carbonyl groups in the rHDPE sample at  $1713.83\text{ cm}^{-1}$ . It is important to note there was no significant change in thermal stability as indicated by TGA-DTG. The findings showed that the flexural strength and impact strength of neat rHDPE and rHDPE-ZF composites significantly decreased along with the weathering time. The flexural modulus of neat rHDPE had

tendency to increase while those of rHDPE-ZF composite decreased along with the exposure time. It was also revealed that alkaline treatment was able to consistently enhance the mechanical properties, specifically the flexural and impact strength during exposure, but its influence on impact strength was eliminated after 2 months of exposure. The SEM examinations of the surface and fracture of composites also showed the growth of gaps between fibers and matrix, breakage of the fiber and matrix bonds, and cracks on the matrix around the fibers. It is important to note the fracture surface of the rHDPE which was originally ductile became more brittle after exposure to weather. Therefore, rHDPE and rHDPE-ZF composites are confirmed to be suitable for indoor

applications, such as partition panels, acoustic panels, car dashboards, and cabin panels, but not recommended for outdoor where there is UV radiation and moisture exposure.

### Acknowledgements

The author expresses gratitude the Indonesian Ministry of Education and Culture for the financial support provided through Research Grant (Contract Number 452/UN27.21/PN/2020).

### Nomenclature

b	specimen width (mm)
d	specimen thickness (mm)
d	diameter of fiber
E <sub>b</sub>	elastic modulus of bending (MPa)
F	maximum bending load (N)
L	distance between two supports (mm)
l <sub>c</sub>	critical length (mm)
y	deflection (mm)
R	distance from the center of pendulum rotation to the center of mass (mm)
W	total energy absorbed (J)
w	pendulum weight (N)

### Greek symbols

$\alpha$	impact strength (J/m <sup>2</sup> )
$\sigma_b$	flexural strength (MPa)
$\sigma_u$	ultimate tensile strength (MPa)
$\alpha^l$	initial angle of swing arm (deg)
$\beta$	rebound angle of swing arm (deg)

### References

- 1) J. Holbery, and D. Houston, "Natural-fibre-reinforced polymer composites in automotive applications," *J Miner*, 58 (11) 80–86 (2006). doi:10.1007/s11837-006-0234-2.
- 2) E. Syafri, Jamaluddin, S. Wahono, A. Irwan, M. Asrofi, N. H. Sari NH, and A. Fudholi, "Characterization and properties of cellulose microfibers from water hyacinth filled sago starch biocomposites," *Int J Biol Macromol*, 137 119-125 (2019). doi:10.1016/j.ijbiomac.2019.06.174.
- 3) T. Gurunathan, S. Mohanty, and S. K. Nayak, "A review of the recent developments in biocomposites based on natural fibres and their application perspectives," *Compos Part A Appl Sci Manuf*, 77 1–25 (2015). doi:10.1016/j.compositesa.2015.06.007
- 4) N. A. Ismail, and M. F. A. Bakar, "Salak - Salacca zalacca," *Exotic Fruits*, Academic Press, 383–390 (2018).
- 5) A. Mahyudin, S. Arief, H. Abral, and Emriadi, "Mechanical Properties and Biodegradability of Areca Nut Fiber-reinforced Polymer Blend Composites," *Evergreen*, 7 (3) 366-372 (2020).
- 6) N. Sgriccia, M. C. Hawley, and M. Misra, "Characterization of natural fiber surfaces and natural fiber composites," *Compos Part A Appl Sci Manuf*, 39 (10)1632–1637 (2008). doi:10.1016/j.compositesa.2008.07.007
- 7) R. A. S. Lestari, W. B. Sediawan, S. Syamsiah, Sarto, and J. A. Teixeira, "Hydrogen sulfide removal from biogas using a salak fruit seeds packed bed reactor with sulfur oxidizing bacteria as biofilm," *J Environ Chem Eng*, 4 (2) 2370–2377 (2016). doi:10.1016/j.jece.2016.04.014.
- 8) M. Ayadi, S. Ahou, S. Awad, and M. Abderrabba, "Production of Biogas from Olive Pomace," *Evergreen*, 7 (2) 228-233 (2020). doi:10.5109/4055224.
- 9) S. P. Dwivedi, M. Maurya, N. K. Maurya, and A. K. Srivastava, "Utilization of Groundnut Shell as Reinforcement in Development of Aluminum Based Composite to Reduce Environment Pollution: a review," *Evergreen*, 7 (1) 15-25 (2020). doi:10.5109/2740937.
- 10) A. F. Ridassepri, F. Rahmawati, K. R. Heliani, and Chairunnisa, "Activated Carbon from Bagasse and its Application for Water Vapor Adsorption," *Evergreen*, 7 (3) 409-416 (2020).
- 11) M. M. Kabir, H. Wang, K. T. Lau, and F. Cardona, "Chemical treatments on plant-based natural fibre reinforced polymer composites: An overview," *Compos Part B Eng*, 43 (7) 2883–2892 (2012). doi:10.1016/j.compositesb.2012.04.053
- 12) W. P. Raharjo, R. Soenoko, A. Purnowidodo, M. A. Chiron, and Triyono, "Mechanical properties of untreated and alkaline treated fibers from zalacca midrib wastes," *AIP Conf Proc*, 1717 1–8 (2016). doi:10.1063/1.4943461.
- 13) W. P. Raharjo, R. Soenoko, A. Purnowidodo, M. A. Chiron, and Triyono, "Effect of alkaline treatment on the characterization of zalacca midrib wastes fibers," *AIP Conf Proc*, 1717 1–8 (2016). doi:10.1063/1.4943462.
- 14) W. P. Raharjo, R. Soenoko, A. Purnowidodo, and M. A. Chiron, "Characterization of sodium-bicarbonate-treated zalacca fibers as composite reinforcements," *Evergreen*, 6 (1) 29–38.
- 15) W. P. Raharjo, R. Soenoko, A. Purnowidodo, and M. A. Chiron, "Influence of several chemical treatment on the interfacial shear strength of zalacca fibres and low-density polyethylene matrix," *AIP Conf Proc*, 2097 (April) 1-8 (2019). doi:10.1063/1.5098181.
- 16) W. P. Raharjo, and R. Soenoko R., "Effect of chemical treatment on wettability of Zalacca fibres as composites reinforcements," *IOP Conf Ser Mater Sci Eng*, 494 (1) 0–8 (2019). doi:10.1088/1757-

- 899X/494/1/012007/meta.
- 17) A. J. Peacock, "Handbook of Polyethylene, Structures, Properties and Applications," Marcel Dekker, 2000.
  - 18) K. B. Adhikary, S. Pang, and M. P. Staiger, "Dimensional stability and mechanical behaviour of wood-plastic composites based on recycled and virgin high-density polyethylene (HDPE)," *Compos Part B Eng*, 39 (5) 807–815 (2007). doi:10.1016/j.compositesb.2007.10.005.
  - 19) P. K. Mallick, "Fiber-Reinforced Composites, Materials Manufacturing and Design," CRC Press, 2007.
  - 20) X. Zhang, Z. Wang, L. Cong, S. Nie, and J. Li, "Effects of Fiber Content and Size on the Mechanical Properties of Wheat Straw/Recycled Polyethylene Composites," *J Polym Environ*, 28 1833–1840. doi:10.1007/s10924-020-01733-8.
  - 21) D. Ariawan, M. S. Salim, R. Mat Taib, M. Z. A. Thirmizir, and Z. A. M. Ishak, "Durability of alkali and heat- treated kenaf fiber/unsaturated polyester composite fabricated by resin transfer molding under natural weathering exposure," *Adv Polym Technol*, 37 1420–1434 (2018). doi:10.1002/adv.21801.
  - 22) A. H. Umar, E. S. Zainuddin, and S. M. Sapuan, "Effect of Accelerated Weathering on Tensile Properties of Kenaf Reinforced High-Density Polyethylene Composites," *J Mech Eng Sci*, 2 198–205 (2012). doi: 10.15282/jmes.2.2012.7.0018.
  - 23) J. K. Pandey, S. H. Ahn, C. S. Lee, A. K. Mohanty, and M. Misra, "Recent advances in the application of natural fiber based composites," *Macromol Mater Eng*, 295 (11) 975–989 (2010). doi:10.1002/mame.201000095.
  - 24) D. Ariawan, T. S. Rivai, E. Surojo, S. Hidayatulloh, H. I. Akbar, and A. R. Prabowo, "Effect of alkali treatment of Salacca Zalacca fiber (SZF) on mechanical properties of HDPE composite reinforced with SZF," *Alexandria Eng J*, 59 (5) 3981–3989 (2020). doi:10.1016/j.aej.2020.07.005.
  - 25) W. W. Raharjo, R. Soenoko, Y. S. Irawan, and A. Suprpto, "The Influence of Chemical Treatments on Cantala Fiber Properties and Interfacial Bonding of Cantala Fiber/Recycled High Density Polyethylene (rHDPE)," *J Nat Fibers*, 15 (1) 98–111 (2018). doi:10.1080/15440478.2017.1321512.
  - 26) W. D. Callister, and D. G. Rethwisch, "Materials Science and Engineering An Introduction," Wiley, 2018.
  - 27) D. Ariawan, Z. A. Mohd Ishak, M. S. Salim, R. Mat Taib, and M. Z. Ahmad Thirmizir, "Wettability and interfacial characterization of alkaline treated kenaf fiber-unsaturated polyester composites fabricated by resin transfer molding," *Polymer Composites*, 38 (3) 507–515 (2015). doi:10.1002/pc.23609.
  - 28) Y. Cao, F. Chan, Y-H, Chui, and H. Xiao, "Characterization of flax fibres modified by alkaline, enzyme, and steam-heat treatments," *BioResources*, 7 (3) 4109–4121 (2012).
  - 29) R. M. Rowell, S. E. Lange, and R. E. Jacobson, "Weathering performance of plant-fiber/thermoplastic composites," *Mol Cryst Liq Cryst Sci Technol Sect A Mol Cryst Liq Cryst*, 353 (1) 85–94 (2006). doi:10.1080/10587250008025650
  - 30) D. G. Goodwin, T. Lai, Y. Lyu, C. Yuan, and A. Campos, "NanoImpact The impacts of moisture and ultraviolet light on the degradation of graphene oxide/polymer nanocomposites," *NanoImpact*, 19 (July) 100249. doi:10.1016/j.impact.2020.100249.
  - 31) I. Mouallif, A. Latrach, M. Chergui, A. Benali, and N. Barbe, "FTIR study of HDPE structural changes , moisture absorption and mechanical properties variation when exposed to sulphuric acid aging in various temperatures," *Polym Degrad Stab*, 29 1–7 (2011).
  - 32) W. Asghar, I. A. Qazi, H. Ilyas, A. A. Khan, M. A. Awan, and M. R. Aslam, "Comparative Solid Phase Photocatalytic Degradation of Polythene Films with Doped and Undoped TiO<sub>2</sub> Nanoparticles," *J Nanomater*, 2011 1–8 (2011). doi:10.1155/2011/461930.
  - 33) T. M. Mower, and V. C. Li, "Fracture Characterization of Random Short Fiber Reinforced Thermoset Resin Composites," *Eng Fract Mech*, 26 (4) 593–603 (1987). doi:10.1016/0013-7944(87)90100-7.